

## Structural Distortions and Electrical Properties of Magnetolectric Layered Perovskites: $\text{Bi}_4\text{Ti}_3\text{O}_{12} \cdot n\text{BiFeO}_3$ ( $n=1\&2$ )

Taegyung Ko, Gyusuk Bang\* and Jungmuk Shin

Department of Ceramic Engineering, Center for Chemical Dynamics,  
Inha University, Incheon 402-751, Korea

\*Present address: Korea Electric Technology Institute, Pyungtaek, 451-860, Korea

(Received October 2, 1997)

The structure refinements and the electrical and magnetolectric measurements were performed for BIT.1BF and BIT.2BF. The tetragonal distortion of the  $ab$  plane became lessened with the addition of  $\text{BiFeO}_3$  into  $\text{Bi}_4\text{Ti}_3\text{O}_{12}$  significantly. However, the tilting of the outer-oxygen octahedra of the perovskite unit and the elongation of the  $(\text{Bi}_2\text{O}_2)^{2+}$  layers became more pronounced. For the both phases, the variations of dielectric properties and electrical conductivities at high temperatures showed that the ferroelectric I - ferroelectric II phase transition existed before reaching the Curie temperature. The electrical conductivity became higher with the increase of  $\text{Fe}^{3+}$  ions, implying that electron transfer increased correspondingly. The magnetolectric effect was observed linear up to  $\sim 8$  kOe, which was stronger in BIT.1BF than BIT.2BF. This behavior indicates that the distortion of the  $ab$  plane may affect the induced polarization as well as magnetic moment.

**Key words:** Magnetolectric,  $\text{Bi}_4\text{Ti}_3\text{O}_{12} \cdot \text{BiFeO}_3$ ,  $\text{Bi}_4\text{Ti}_3\text{O}_{12} \cdot 2\text{BiFeO}_3$ , Structure refinement, Electrical properties, Magnetolectric effect

### I. Introduction

A series of  $\text{Bi}_4\text{Ti}_3\text{O}_{12} \cdot n\text{BiFeO}_3$  (BIT.nBF) are ferroelectrics with a layer structure, allowing various numbers of the perovskite structural unit of  $\text{BiFeO}_3$  to add into  $\text{Bi}_4\text{Ti}_3\text{O}_{12}$ . Such an accommodation will not distort the structural integrity of  $\text{Bi}_4\text{Ti}_3\text{O}_{12}$  severely by having commensurate displacive modulations of constituent atoms. For  $\text{Bi}_4\text{Ti}_3\text{O}_{12}$ , various co-operative physical properties could be concocted with adding a number of either  $\text{BiFeO}_3$  or other  $\text{ABO}_3$ . In structure, a number of the perovskite units are interleaved with the  $(\text{Bi}_2\text{O}_2)^{2+}$  layers. Ismailzade *et al.*<sup>1)</sup> showed that BIT.1BF, BIT.2BF, and BIT.5BF have orthorhombic distortion in common. When a slab of  $\text{BiFeO}_3$  is permitted in the perovskitic layers, the  $c$ -dimension will expand and the chains of the oxygen octahedra of the perovskitic layers become lesser constrained between  $(\text{Bi}_2\text{O}_2)^{2+}$  layers. As a consequence, various modes of the atomic displacement could be easier to occur. Three major displacive modes<sup>2)</sup> in BIT.nBF may exist: the  $F2mm$  mode (the atomic shifts along the  $a$ -axis); the  $Bmab$  or  $Amam$  mode (the Ti-octahedral rotation along the  $a$ -axis); the  $Bbab$  or  $Bbam$  mode (the Ti-octahedral rotation along the  $c$ -axis).

BIT.nBF has been reported to be magnetolectric.<sup>3,4)</sup> In magnetolectrics, magnetic moment can be induced by electrical field or vice versa. For instance, a weak ferromagnetism was proved to be entirely induced by ferroelectricity in  $\text{BaMnF}_4$ .<sup>5)</sup> Electrical signal by applying magnetic field was observed for BIT.1BF<sup>3)</sup> and BIT.5BF<sup>4)</sup>.

Deverin<sup>6)</sup> mentioned that BIT.1BF could show a similar behavior like  $\text{BaMnF}_4$ . Among the BIT.nBF compounds, BIT.5BF containing the highest amount of  $\text{Fe}^{3+}$  exhibited a rather weakest electrical signal by applying magnetic field.<sup>4)</sup> A Mössbauer study<sup>6)</sup> suggested that BIT.5BF may have superparamagnetism for such a weak magnetolectricism, which could be resulted from isolated perovskitic sublayers containing iron ions separated by diamagnetic ion-containing layers. At present, the origin of the magnetolectric effect in BIT.nBF is not clearly known yet. However, it appeared to be related to various cation orderings related to  $\text{Fe}^{3+}$  as well as structural distortions induced by the addition of  $\text{BiFeO}_3$  into  $\text{Bi}_4\text{Ti}_3\text{O}_{12}$ . In this study, we have investigated the structural distortions and the electrical and magnetolectric properties associated with BIT.1BF and BIT.2BF varying the number of  $\text{BiFeO}_3$ .

### II. Experimentals

#### 1. Powder X-ray diffraction

$\text{Bi}_4\text{Ti}_3\text{O}_{12} \cdot n\text{BiFeO}_3$  ( $n=1\&2$ ) were prepared by solid state reaction using  $\text{Bi}_2\text{O}_3$  (Aldrich 99.99%),  $\text{Fe}_2\text{O}_3$  (Aldrich, 99.98%), and  $\text{TiO}_2$  (Aldrich, 99.99%) as starting reagents. The stoichiometric mixtures were fired twice at  $900^\circ\text{C}$  in air for 12 hrs with an intermediate regrinding. After the second firing, the compounds were lightly crushed and sieved to  $<45 \mu\text{m}$ . Powder X-ray diffraction data were collected using HRPD with Bragg-Brentano geometry on 3C 2 beam line at the Pohang Light Source, which was

operated at 2 GeV with the average beam current of ~100 mA. The energy resolution of HRPD as  $\Delta\lambda/\lambda$  was  $5 \times 10^{-4}$ . Energy calibration was carried out using CoK absorption edge and then a wavelength was set at 1.78395 Å. Data collection was carried out with a constant step size of  $0.02^\circ$  and the count time of 2~3s for the  $2\theta$  range of  $6\text{--}68^\circ$ .

## 2. Structure refinements

Rietveld refinements were carried out using the program DBWS-9411.<sup>7)</sup> A peak shape function used was the Pearson VII with a refineable variable independent of  $2\theta$ . The angular dependence of FWHM was refined with the three U, V, and W parameters. For diminishing the peak overlap, intensities within eight times of the full width at FWHM were considered to contribute to a calculated profile. Each trial model for the both structures was derived from a prototype structure of a space group of  $I4/mmm$ . Based on the systematic absences in the powder diffractions, the space group of BIT.nBF was assumed to be either  $A2_1am$  for  $n=1$  or  $B2cb$  for  $n=2$ . The expected R-value of the refinement was ~19%, indicating a complexity of the both structures compared to the total number of data points. As a result, a lack of high angle data led us to constrain the  $(x,y)$  of the constituent atoms to the corresponding atomic positions of the prototype structure with an isotropic temperature model. In addition, the temperature factors of the all oxygen atoms were fixed to be 1.0. Such a reduction of the refineable structure parameters resulted in a stable convergence with the final  $R \sim 15\%$ ,  $R_{wp} \sim 21\%$ , and goodness of fit  $\sim 1.1$ . Considering the expected R value, any further refinement would not be attempted. The refined structure data of BIT.1BF and BIT.2BF were summarized in Table 1 and Table 2, respectively.

## 3. Electrical and magnetoelectric measurements

For the measurements of dielectric and magnetoelec-

**Table 1.** Structural Parameters for  $\text{Bi}_4\text{Ti}_5\text{O}_{13} \cdot 1\text{BiFeO}_3$

Atom	X	Y	Z	$B_{iso}(\text{\AA}^2)$
O1	0.2500	0.2500	0.0000	1.0000
O3	0.2500	0.2500	0.0954(8)	1.0000
O4	0.2500	0.2500	0.1898(9)	1.0000
(Ti, Fe)1	0.2500	0.2500	0.0493(4)	9.02(1)
(Ti, Fe)2	0.2500	0.2500	0.1505(4)	6.08(1)
O5	0.0000	0.0000	0.0494(14)	1.0000
O6	0.5000	0.5000	0.0502(15)	1.0000
O7	0.0000	0.0000	0.1586(13)	1.0000
O8	0.5000	0.5000	0.1433(11)	1.0000
Bi1	0.2500	-0.2500	0.0000	7.1(30)
Bi2	0.2500	-0.2500	0.1052(1)	6.1(18)
Bi3	0.2500 <sup>†</sup>	-0.2500	0.2183(1)	8.6(21)
O2	0.0000	0.0000	0.2433(17)	1.0000

<sup>†</sup> fixed parameter.

orthorhombic : Space group  $A2_1am$

$a=5.4786(1)$ ,  $b=5.4484(1)$ ,  $c=41.2941(7)$

$R_{Bragg}=7.85\%$ ,  $R_p=15.20\%$ ,  $R_{wp}=21.63\%$ ,  $S=1.17$

**Table 2.** Structural Parameters for  $\text{Bi}_4\text{Ti}_5\text{O}_{13} \cdot 2\text{BiFeO}_3$

Atom	X	Y	Z	$B_{iso}(\text{\AA}^2)$
O1	0.0000	0.0000	0.3177(15)	1.0000
O3	0.0000	0.0000	0.3813(9)	1.0000
O4	0.0000	0.0000	0.4582(11)	1.0000
O5	0.2500	0.2500	0.0000	1.0000
Ti1	0.0000	0.0000	0.5000	35(2)
Ti2	0.0000	0.0000	0.4145(6)	12(1)
Fe1	0.0000	0.0000	0.3278(5)	5(1)
O6	0.2500	0.2500	0.0843(12)	1.0000
O7	0.7500	0.7500	0.0770(12)	1.0000
O8	0.2500	0.2500	0.1549(13)	1.0000
O9	0.7500	0.7500	0.1654(14)	1.0000
Bi1	0.0000	0.0000	0.0424(1)	6.5(2)
Bi2	0.0000	0.0000	0.1305(1)	6.2(3)
Bi3	0.0000 <sup>†</sup>	0.0000	0.2198(1)	16.3(4)
O2	0.2500	0.2500	0.2621(10)	1.0000

<sup>†</sup> fixed parameter.

orthorhombic : Space group  $B2cb$

$a=5.4972(2)$ ,  $b=5.4723(2)$ ,  $c=49.4984(21)$

$R_{Bragg}=8.84\%$ ,  $R_p=15.20\%$ ,  $R_{wp}=21.20\%$ ,  $S=1.08$

tric properties, powders of BIT.1BF and BIT.2BF were separately prepared using the sol-gel process to obtain a better densification. For the synthesis,  $\text{Bi}(\text{CH}_3\text{COO})_3$ ,  $\text{Fe}(\text{NO}_3)_3 \cdot 9\text{H}_2\text{O}$  (Junsei, min. 98%), and  $\text{Ti}(\text{OC}_2\text{H}_5)_4$  (Aldrich, 97%) were used as precursors. Glacial acetic acid and 2-methoxyethanol were selected for solvents.  $\text{Bi}(\text{CH}_3\text{COO})_3$  was synthesized from the reaction of  $\text{Bi}_2\text{O}_3$  (Shinyo, max. 99.5%) and glacial acetic acid, whose purity gravimetrically determined was ~99.9%.  $\text{Ti}(\text{OC}_2\text{H}_5)_4$  was diluted with 2-methoxyethanol and put into alcohol exchange reaction.  $\text{Bi}(\text{CH}_3\text{COO})_3$  and  $\text{Fe}(\text{NO}_3)_3 \cdot 9\text{H}_2\text{O}$  were dissolved into glacial acetic acid. All the metal solutions were mixed, refluxed, and vacuum-distilled to produce a complex alkoxide powder, which finally was dissolved to be 0.05 M by 2-methoxyethanol. Sols were obtained from hydrolysis with water of 180 moles times those of Bi acetate, aged at room temperature, dried at  $125^\circ\text{C}$ , and finally pyrolyzed at  $700^\circ\text{C}$  for 1 hr. The products were uniaxially pressed into pellets of 10 mm in dia. and 2 mm thick under  $1 \text{ ton/cm}^2$ , which were sintered at  $1000^\circ\text{C}$  for 2 hrs. After polishing and etching the surfaces of the sintered pellets with 1:1 conc.  $\text{HNO}_3$  and HF (10%) solution, their microstructures were observed by SEM. The dielectric properties and DC conductivities were measured with an HP4192A impedance analyzer and HP3466A digital multimeter, respectively in a temperature-controlled furnace. Magnetoelectric measurements were conducted in a parallel configuration<sup>4)</sup> where the polarization and the magnetization were normal to the plane of the specimen using Keithley 617 programmable electrometer and Riken Denshi BHU-60 electromagnet.

## III. Results and Discussion

### 1. Structural distortions

The structures of BIT.1BF and BIT.2BF based on the refined data were presented in Fig. 1, where the struc-

ture of  $\text{Bi}_4\text{Ti}_3\text{O}_{12}$  was also given for comparison. In BIT.  $n\text{BF}$ , one layer consists of  $(\text{Bi}_2\text{O}_2)^{2+}$ , in which  $\text{Bi}^{3+}$  ions show a steric effect on bonding due to lone paired electrons. The other layer is the perovskitic unit of  $\text{Bi}_{m-1}(\text{Ti}, \text{Fe})_m\text{O}_{3m+1}$  ( $m=3+n$ ), in which  $\text{Bi}^{3+}$  ions seem to act like spherical ions. The perovskitic layers can be multiplied, depending on the number of the added  $\text{BiFeO}_3$  ( $n$ ), which resulted in changing the lattice dimensions. The variations of  $c/b$  and  $a/b$  were shown in Fig. 2 and Fig. 3, respectively. The  $c/b$  ratio increased quite linearly, while the  $a/b$  ratio decreased. The variation of the lattice dimensions indicates that the greater structural complexity tends to reduce the degree of the atom displacements in the basal plane. Our previous study<sup>9)</sup> showed that the  $\text{Bi}^{3+}$  ions of the perovskitic layers may cause an abnormal expansion of the  $a$ -dimension in  $\text{Bi}_4\text{Ti}_3\text{O}_{12}$  ( $n=0$ ), which may be related to the steric effect of the  $\text{Bi}^{3+}$  ions along the  $a$ -axis. Therefore, it can be considered that the  $\text{Bi}^{3+}$  ions become less stereo-active as the number of  $n$  increases. As the greater structural distortion of the basal plane is related to the higher spontaneous polarization in the Aurivillius phases,<sup>9)</sup> such a reduction may not result a higher ferroelectricity. In contrast, the  $(\text{Bi}_2\text{O}_2)^{2+}$  layers appeared to be more distorted along the  $c$ -axis with the addition of  $\text{BiFeO}_3$ , which is shown in Fig. 1. The  $c$ -axis expansion may reflect a substantial change in the stereo-active bonding of the  $\text{Bi}^{3+}$  ions of the  $(\text{Bi}_2\text{O}_2)^{2+}$  layers along the  $c$ -axis. However, considering that the  $(x,y)$  parameters of the atoms are constrained in our structural refinements, such a distortion could not be well defined.

The addition of  $\text{BiFeO}_3$  may result in disordering of the octahedrally coordinated Ti and Fe atoms in the perovskitic layers. For  $n=1$ , the symmetry element of  $m$  in  $A2_1am$  lies at the middle of the perovskitic slab. An

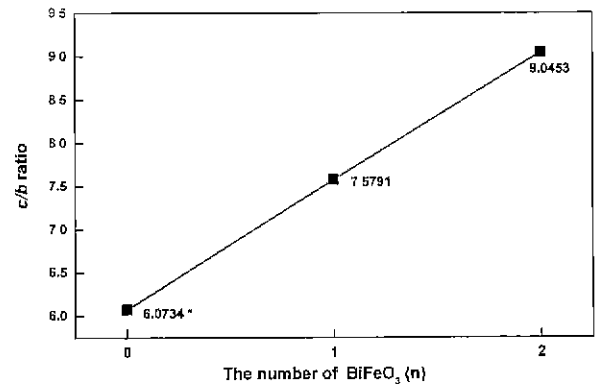


Fig. 2. Lattice distortions of  $\text{Bi}_4\text{Ti}_3\text{O}_{12} \cdot n\text{BiFeO}_3$  depending on  $n$ . <sup>9)</sup>from Rae *et al.*(1990).

ordered arrangement of the Ti and Fe atoms may not be possible for BIT.1BF. In contrast, such an ordering could exist for  $n=2$ , even though  $n$  glide exists at the center of

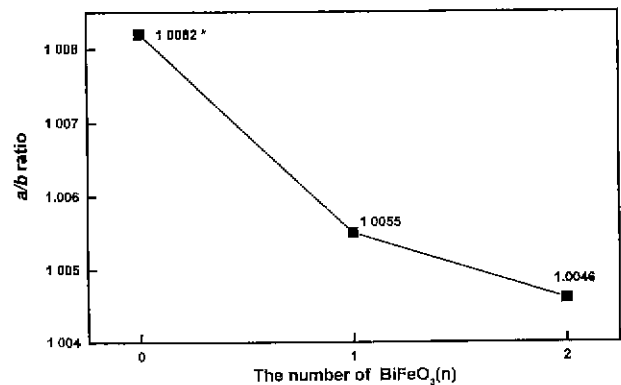


Fig. 3. Lattice distortions of  $\text{Bi}_4\text{Ti}_3\text{O}_{12} \cdot n\text{BiFeO}_3$  depending on  $n$ . <sup>9)</sup>from Rae *et al.*(1990).

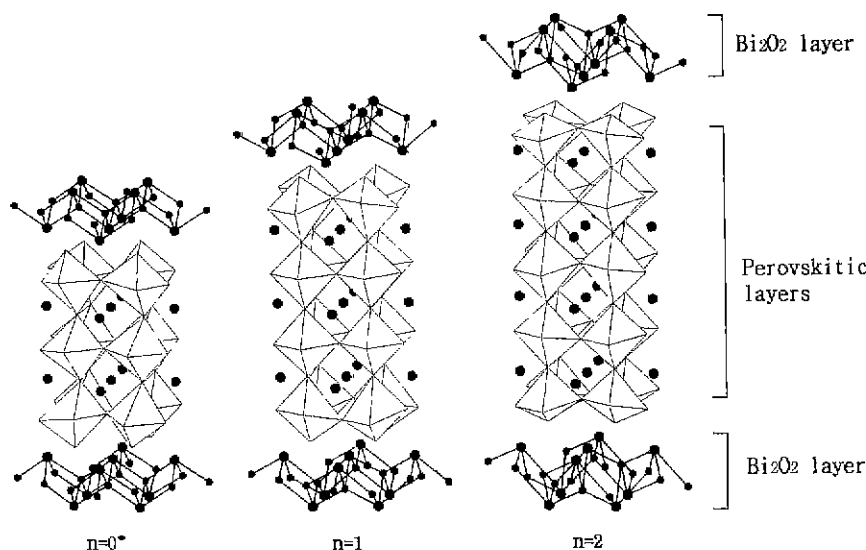


Fig. 1. Crystal structures of  $\text{Bi}_4\text{Ti}_3\text{O}_{12} \cdot n\text{BiFeO}_3$  showing the layer structure perpendicular to  $[110]$ . Bismuth atoms are shaded dark grey (●) and oxygen atoms are solid black (●). <sup>9)</sup> from Rae *et al.*(1990).

the *B*-centered cell. For BIT.2BF, several models were tested for the atomic arrangements of Ti and Fe during the structural refinement. By fixing the (*x,y*) parameters of the atoms, the isotropic temperature factors of the Fe and Ti atoms tended to be highly positive during our structural refinement. However, the thermal factors of these atoms in the inner octahedra appeared to be sensitive to the presence of disordering. In our refinement, an ordered atomic arrangement ensured a lower thermal factor ( $B_{iso}=35\sim41$ ) than the disordered one did ( $B_{iso}=54\sim69$ ).

In addition, the distortion of Ti-octahedra differs sensitively depending on *n*. Although the displacive atomic modulations were only partially deduced, the general feature of the Ti-octahedra indicated that the outer octahedra appeared to be more seriously compressed as *n* increases, compared to the central ones. Such a distortion is related to the *Amam* mode for *n*=1 and the *Bmab* mode for *n*=2, which is responsible for the rotation of the Ti-octahedra along the *a*-axis. The increase of the outer-octahedral distortion was associated with the strained  $(\text{Bi}_2\text{O}_2)^{2+}$  layers, indicating that the tilting of the Ti-octahedra was somewhat adjusted by the distortion of the  $(\text{Bi}_2\text{O}_2)^{2+}$  layers. Considering the linear increase of the *c/b* ratio, the higher outer-octahedral compression needs to be compensated by the bigger expansion of the  $(\text{Bi}_2\text{O}_2)^{2+}$  layers along the *c*-axis. Otherwise, the increase of *n* may result in the relaxation of the perovskitic layers along the *c*-axis. At present, further data collections to the high angles are planned to complete the Rietveld refinements for BIT.1BF and BIT.2BF. The use of a shorter wavelength may be required to avoid the serious absorption due to the  $\text{Bi}^{3+}$  ions.

## 2. Microstructures

Fig. 4a and 4b presented the SEM photographs of BIT.1BF and BIT.2BF, which were prepared at 700°C for 1 hr. Their grains had platelike forms. At 1000°C, when they were sintered for 2 hrs, strong grain growth occurred. Fig. 4c and 4d showed that there was a strong growth of the major plane of the platelike grains perpendicular to the *c*-axis during the sintering. A full densification would not reach successfully due to the anisotropic grain growth. A similar behavior was mentioned for  $\text{Bi}_4\text{Ti}_5\text{O}_{12}$ .<sup>10)</sup>

## 3. Dielectric properties

The dielectric constants( $\epsilon$ ) and losses( $\tan\delta$ ) of BIT.1BF and BIT.2BF were measured in a range of 100 Hz~13 MHz, which were shown in Fig. 5 and 6, respectively. The dielectric constants were ~110 and did not show strong frequency dispersion in a range of 100 kHz~10 MHz. However, the dielectric constant of BIT.1BF increased a rather steeply at lower frequencies, compared to that of BIT.2BF. For the layered phases, as the size of *c*-dimension increases, octahedral chains containing  $\text{Ti}^{4+}$

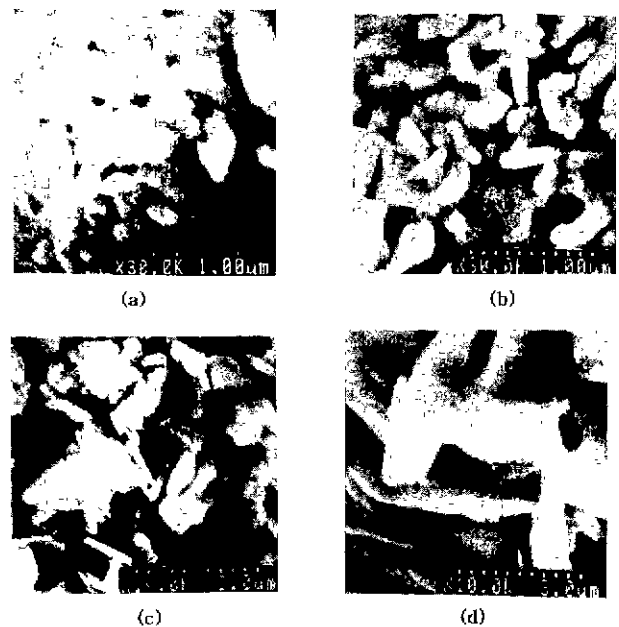


Fig. 4. SEM photographs of BIT · nBF(*n*=1~2) powders pyrolyzed for 1hr; (a) *n*=1, (b) *n*=2 at 700°C, (c) *n*=1 and (d) *n*=2 at 1000°C.

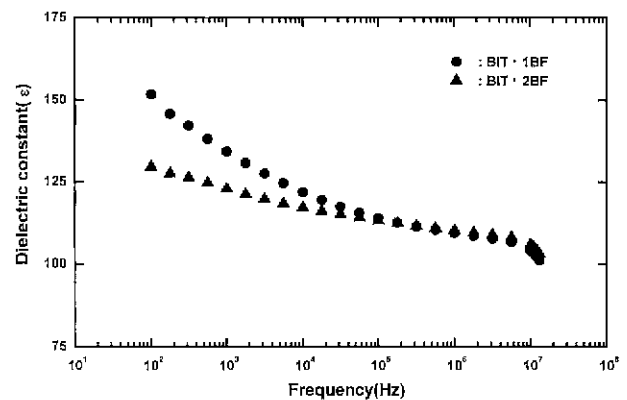


Fig. 5. Dielectric constants of BIT · nBF(*n*=1~2) as a function of frequency.

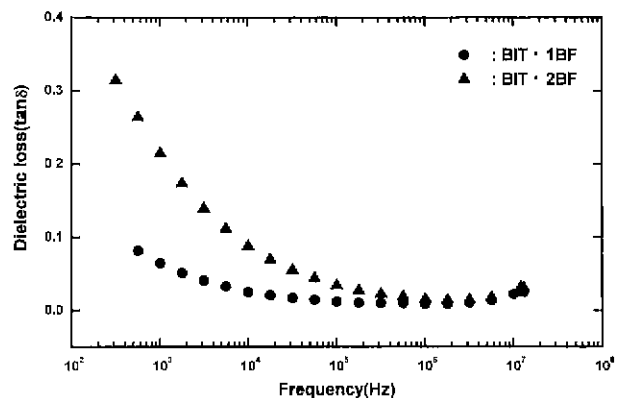


Fig. 6. Dielectric losses of BIT · nBF(*n*=1~2) as a function of frequency.

and  $\text{Fe}^{3+}$  become larger. Dipolar response of such a larger cluster could be slower. The low frequency dispersion of the dielectric constant could be weaker in BIT.2BF. Furthermore, the dielectric losses increased at a larger step in BIT.2BF, at lower frequencies. This behavior again implies that the bigger cluster of the octahedral chains might be strongly relaxed.

The dielectric properties of BIT.1BF and BIT.2BF at high temperatures were presented in Fig. 7 and 8, respectively. In general, those values became smaller at higher frequencies. The dielectric constants and losses increased steeply at  $300^\circ\text{C}\sim 400^\circ\text{C}$ . According to Deverin,<sup>3</sup> a magnetic ordering might be responsible for these changes. For the both phases, as magnetic moment is correlated to the magnitude of polarization, any change in magnetic ordering should cause a dielectric change. In addition, the onset of the magnetic ordering may cause a change in electrical conductivity.<sup>3</sup> However, a similar result<sup>11</sup> on BIT was also reported, in that the increase of dielectric constant and dielectric loss around that temperature range might correspond to the increase of AC electric conductivity. The broad anomalies observed around  $400^\circ\text{C}$  for the both phases therefore may not be related solely to the magnetic ordering.

At the higher temperatures, two maxima were observed at the  $\epsilon$ -T curves of the both phases. It has been

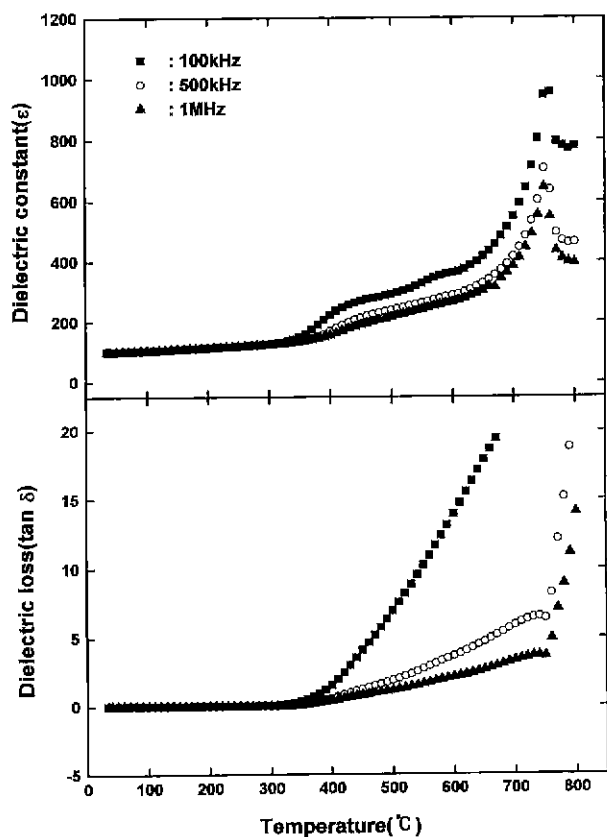


Fig. 7. Dielectric constant and loss vs. temperature of BIT 1BF.

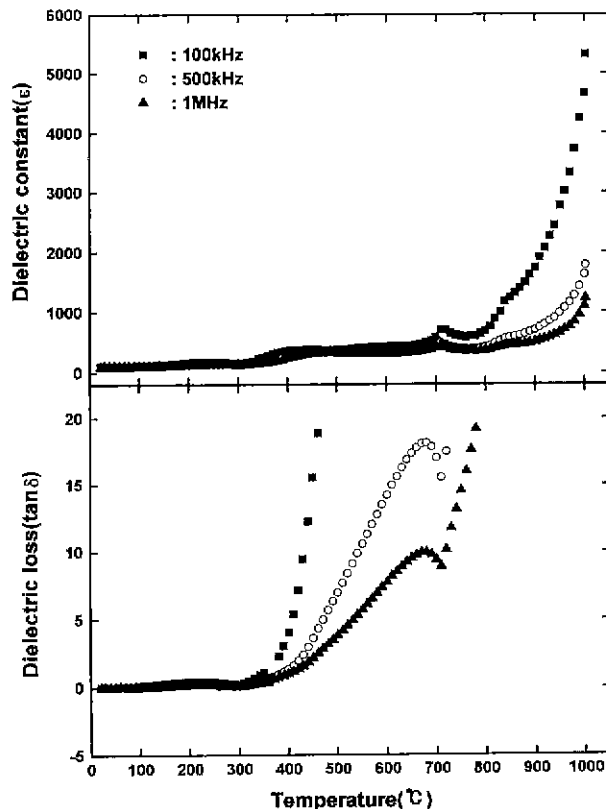


Fig. 8. Dielectric constant and loss vs. temperature of BIT 2BF.

known that a Curie temperature was about  $750^\circ\text{C}$ <sup>13</sup> for BIT.1BF, while it was either  $\sim 807^\circ\text{C}$ <sup>12</sup> or  $898^\circ\text{C}$ <sup>3</sup> for BIT.2BF. In this study, the Curie temperature of BIT.1BF was  $750^\circ\text{C}$ , which agreed well with the reported value. For BIT.2BF, a Curie temperature was observed at  $845^\circ\text{C}$ . Deverin<sup>3</sup> reported that there was one more transition point at  $752^\circ\text{C}$  for BIT.2BF, which was related to a ferroelectric-ferroelectric phase transition. Our study confirmed that a similar transition was observed to occur at  $710^\circ\text{C}$  for BIT.2BF and  $580^\circ\text{C}$  for BIT.1BF. Therefore, for the both phases, a sequence of phase transition suggested by Deverin<sup>3</sup> could be established: Ferroelectric II-Ferroelectric I-paraelectric. In particular, the ferroelectric I-paraelectric transition of BIT.1BF and the ferroelectric I-II transition of BIT.2BF were well defined by pronounced dips in the curves of  $\tan\delta$ -T. The ferroelectric I-II transition of BIT.1BF and the ferroelectric II-paraelectric transition of BIT.2BF were not well defined in the curves of  $\tan\delta$ -T, which might be due to poor contact between the electrode and the specimen at higher temperatures. Our study suggests that the Curie temperature of BIT.nBF increases as n increases.  $\text{Bi}_4\text{Tl}_3\text{O}_{12}$  has the Curie temperature of  $675^\circ\text{C}$ .<sup>13</sup> Subbarao<sup>13</sup> suggested that the lower lattice distortion possessed the higher Curie temperature. As the  $a/b$  ratio decreased as a sequence of BIT, BIT1BF, and BIT2BF, it could be used as a measure of structural distortion for the lay-

ered perovskite phases.

#### 4. Electrical conductivities

DC conductivities were measured against temperatures. In Fig. 9, an Arrhenius format was adopted to show the behaviors of  $\log(\sigma)$  vs.  $1/T$  for BIT.1BF and BIT.2BF. The activation energies ( $E_a$ ) were calculated from this plot. As observed in Fig. 6, four regions could be recognized. Each region with a different activation energy was associated with the similar slope for the both phases. Around 400°C, a distinct change in slope was observed, which were related to the onset of a magnetic ordering.<sup>3)</sup> Using the  $\log(\sigma)$  vs.  $1/T$  below 400°C, the calculated  $E_a$  were 1.82 eV for BIT.1BF and 1.35 eV for BIT.2BF. These values suggest that the electrical conductance increases with the addition of  $\text{BiFeO}_3$  into  $\text{Bi}_4\text{Ti}_3\text{O}_{12}$ . For  $\text{Fe}^{3+}$ -containing compounds, electron transfer can occur between  $\text{Fe}^{3+}$  and  $\text{Fe}^{2+}$ , if oxygen vacancy exists. Such transfer would increase as the amount of  $\text{Fe}^{3+}$  with lowering the activation energy.

The ferroelectric I-II transition could be responsible for the region below  $\sim 750^\circ\text{C}$ . The plots showed, however, that this transition did not cause a pronounced variation in the electrical conductance. In  $\text{Bi}_4\text{Ti}_3\text{O}_{12}$ , the ferroelectric-paraelectric transition did not affect electrical conductance.<sup>14)</sup> The change of the slopes observed in the curves of  $\log(\sigma)$  vs.  $1/T$  at the higher temperatures seemed to be ascribed to the other possibilities on electrical conductance mechanism.

#### 5. Magnetoelectric properties

Magnetoelectric effect was measured by the electrical field induced in the specimen as a capacitor by applying magnetic field. Although DC field was used, electric moment induced by magnetic field ( $\text{ME}_{\text{II}}$ ) could be detected, indicating that the intrinsic time constant of  $\text{ME}_{\text{II}}$  was not small, which was conjectured by Deverin.<sup>3)</sup> Our results were shown Fig. 10. The linear behaviour of  $\text{ME}_{\text{II}}$  was observed at least up to  $\sim 8$  kOe. The coefficients ( $\beta$ ) of  $\text{ME}_{\text{II}}$  calculated from  $E = \beta H$ <sup>4)</sup> were 2.23 V/A and 1.13 V/A for

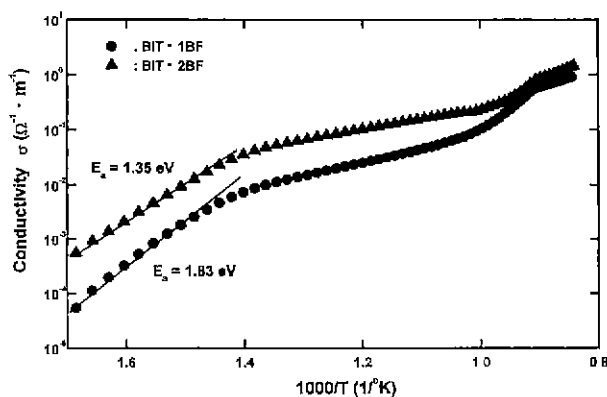


Fig. 9. Temperature dependence of conductivity  $\sigma$  in BIT.nBF ( $n=1\sim 2$ ).

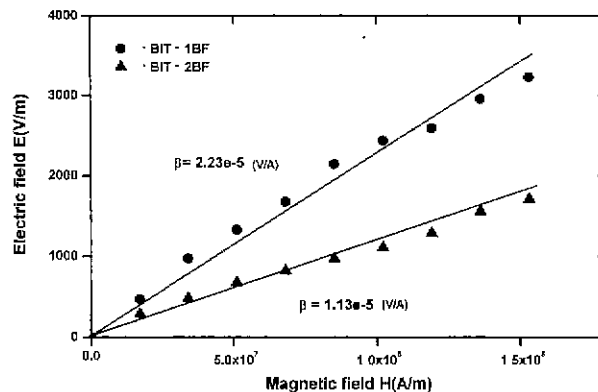


Fig. 10. Variations of electric field vs. magnetic field in BIT.nBF ( $n=1\sim 2$ ).

BIT.1BF and BIT.2BF, respectively. The  $\text{ME}_{\text{II}}$  effect appeared to be larger as the structural distortion such as the  $a/b$  ratio became larger, which was implying that the major magnetic moment lies on the  $ab$  plane.

BIT.2BF<sup>3)</sup> was suggested ferromagnetic. However, Mössbauer measurements on Sn-doped BIT.3BF<sup>15)</sup> and BIT.5BF<sup>6)</sup> showed that they were antiferromagnetic or superparamagnetic. Based on the above results, BIT.1BF seemed to be antiferromagnetic, while BIT.2BF could be very weakly ferromagnetic or better described as superparamagnetic. Considering the crystal symmetries of BIT.1BF and BIT.2BF, the possible magnetic point groups<sup>3,5)</sup> are  $m'm'2$  where  $P_s \parallel |2| \parallel M_s$  or  $m'm'2'$ , where  $P_s \parallel |2$  and  $M_s \perp m$  ( $P_s$  and  $M_s$  being spontaneous polarization and magnetization, respectively). If the magnetic point group belongs to  $m'm'2'$ , the ferroelectric spin canting may be allowed, which results in a ferroelectrically induced ferromagnetism. Cation ordering between  $\text{Fe}^{3+}$  and  $\text{Ti}^{4+}$  might exist in BIT.2BF. BIT.2BF could be considered to be more or less magnetically ordered. Deverin<sup>3)</sup> suggested that BIT.2BF has the magnetic point group of  $m'm'2'$ . Considering the symmetry of BIT.1BF,  $\text{Fe}^{3+}$  and  $\text{Ti}^{4+}$  should be disordered in octahedral chains along the  $c$ -axis. Although it is not clear that BIT.1BF may have the same magnetic point group as BIT.2BF does, considering the larger value of  $\beta$  for BIT.1BF, the higher structural distortion rather than cation ordering might induce the greater spin canting.

## IV. Conclusions

From the structural analysis on BIT.1BF and BIT.2BF, it was observed that the structural distortion of the  $ab$  plane decreased with increasing the number of  $\text{BiFeO}_3$ . Such a reduction may result lowering ferroelectricity in the phase of  $n=2$ . In contrast, the outer-octahedra of the perovskitic layers and the  $(\text{Bi}_2\text{O}_2)^{2+}$  layers appeared to be more distorted for  $n=2$ . In addition, although  $\text{Fe}^{3+}$  and  $\text{Ti}^{4+}$  have been assumed disordered in BIT.nBF, our refinement showed a possibility of the two cations could be

ordered in BIT.2BF. The increase of  $n$  would not result in changing significantly the dielectric properties in the frequency range of 10 kHz~10 MHz. However, at lower frequencies, a low dispersion of the dielectric constant was observed for BIT.2BF, indicating that as the  $c$ -dimension increased, dipolar response of the octahedra cluster became slower. A broad variation of the dielectric constants at 400°C which could be related to the onset of the magnetic ordering, was observed in a series of magnetoelectric BIT. $n$ BF. The Curie temperature of BIT.2BF was higher than that of BIT.1BF, suggesting that the Curie temperature of BIT. $n$ BF increases with  $n$ . The electrical conductance became higher with the increase of  $n$ , which was consistent with the greater amount of  $\text{Fe}^{3+}$  ions. The magnetoelectric behavior of the both phases appeared to be linear under magnetic field. The  $\text{ME}_H$  coefficient became smaller for  $n=2$ , which was matched with the decrease of the tetragonal distortion.

### Acknowledgment

This research was sponsored in part by Korea Science and Engineering Foundation (KOSEF 951-0803-020-1).

### References

1. I. G. Ismailzade, V. I. Nesterenko, F. A. Mirishli and P. G. Rustamov, "X-Ray and Electrical Studies of The System  $\text{Bi}_4\text{Ti}_5\text{O}_{12}\text{-BiFeO}_3$ ", *Sov. Phys. Cryst.*, **12**(3), 400-404 (1967).
2. R. L. Withers, J. G. Thompson and A. D. Rae, "The Crystal Chemistry Underlying Ferroelectricity in  $\text{Bi}_4\text{Ti}_5\text{O}_{12}$ ,  $\text{Bi}_3\text{TiNbO}_9$ , and  $\text{Bi}_2\text{WO}_6$ ", *J. Solid State Chem.*, **94**, 404-417 (1991).
3. J. A. Deverin, "Dielectric and Magnetoelectric Properties of  $\text{Bi}_3\text{Bi}_4\text{Fe}_2\text{Ti}_3\text{O}_{18}$ ", *Ferroelectrics*, **19**, 9-14 (1978).
4. I. H. Ismailzade, R. G. Yakupov and T. A. Melik-Shanzarova, "The Magnetoelectric Effect in Ferroelectric-Antiferromagnetic  $\text{Bi}_5\text{Bi}_1\text{Ti}_1\text{Fe}_6\text{O}_{27}$ ", *Phys. Stat. Sol.*, K85-K87 (1971).
5. D. L. Fox and J. F. Scott, "Ferroelectrically Induced Ferromagnetism", *J. Phys. C:Solid Phys.*, **10**, L329-L321 (1977).
6. S. A. Kizhaev, G. D. Sultanov and F. A. Mirishli, "Magnetic Properties and Meissner Effect in Ferroelectric  $\text{Bi}_5\text{Ti}_1\text{Fe}_6\text{O}_{27}$ ", *Sov. Phys. Solid State*, **15**(1), 214-216 (1973).
7. R. A. Young, A. Sakthivel, T. S. Moss and C. O. Paiva-Santos, "User's Guide to Program DBWS-9411", *Georgia Inst. Tech.*, Atlanta (1994).
8. A. D. Rae, J. G. Thompson, R. L. Withers and A. C. Willis, "Structure Refinement of Commensurately Modulated Bismuth Titanate,  $\text{Bi}_4\text{Ti}_5\text{O}_{12}$ ", *Acta Crystallogr.*, **B46**, 474-487 (1990).
9. T. Ko and H. G. Kang, "Structural Changes of  $\text{Bi}_{4-x}\text{Nd}_x\text{Ti}_5\text{O}_{12}$  ( $x=0-2$ ) Induced by Nd-Substitution", *Pohang Accelerator Laboratory Annual Report*, 107-108 (1996).
10. Y. Inoue, T. Kimura and T. Yamaguchi, "Sintering of Plate-Like  $\text{Bi}_4\text{Ti}_5\text{O}_{12}$  Powders", *Cer. Bull.*, **62**(6), 704-707 (1983).
11. A. Fouskova and L. E. Cross, "Dielectric Properties of Bismuth Titanate", *J. Appl. Phys.*, **41**(7), 2834-2838 (1970).
12. T. Mitsui and S. Nomura, "Ferroelectrics and Related Substances, Subvolume a: Oxides", *Landolt-Bornstein*, ed. K.-H. Hellwege and A.M. Hellwege, Vol. 16 (1981).
13. E. C. Subbarao, "Systematics of Bismuth Layer Compounds", *Int. Ferroelect.*, **12**, 33-41 (1996).
14. J. A. Deverin, "Some Peculiar Properties of Bismuth Titanate", *Ferroelectrics*, **23**, 51-56 (1980).
15. G. D. Sultanov, N. G. Guseinov, R. M. Mirzababaev and F. A. Mirishli, "Superparamagnetism of A Layered Ferroelectric Antiferromagnet  $\text{Bi}_7\text{Ti}_{15}\text{Sn}_{0.6}\text{Fe}_3\text{O}_{31}$ ", *Sov. Phys. Solid State*, **18**(9), 1496-1497 (1976).